Design and Performance of the IceCube Electronics

R. Stokstad, for the IceCube Collaboration

Lawrence Berkeley National Laboratory, Berkeley, CA 94720 USA
rgstokstad@lbl.gov

Abstract

The first sensors of the IceCube Neutrino Observatory were deployed at the South Pole in January, 2005: sixty modules uniformly spaced on one string at depths from 1450 to 2450 meters and sixteen modules in eight tanks at the surface. PMT waveforms are digitized and time-stamped in the modules. This decentralized digital system architecture permits high quality data to be collected with simple twisted-pair copper wires over distances up to 3 km. An overview of the real-time electronics for IceCube is presented here. The performance of the system, determined with calibration sources and cosmic-ray muons, meets expectations. Photon arrival times are determined to a precision of three nanoseconds relative to a master clock on the surface.

I. Introduction

To date, the only neutrinos clearly originating outside the solar system that have been detected are those from SN 1987a. Yet the detection of cosmic rays at energies up to 10^{20} eV indicates there should be a corresponding flux of High Energy neutrinos. The goal of H.E. ν astronomy is the discovery of neutrino fluxes produced by a variety of potential sources, some of which must also produce the H.E. cosmic rays. In essence, this is a "discovery field" where surprises are likely as a part of "mapping the high energy neutrino sky."

The telescopes for H. E. Neutrino Astronomy require that optical sensors be deployed over large volumes of water (because of the low neutrino interaction rate) and at large depths (because of the cosmic-ray muon background). This invariably leads to an array of photomultiplier tubes, each inside a glass pressure sphere and located a long distance from the site where the combined signals are subjected to high-level triggers. While all H.E. ν telescopes have these two features in common, the design solutions for the signal-processing electronics may vary considerably depending on whether the medium is water or ice, and on the logistics of the particular site. The electronics for IceCube, a telescope under construction at the Amundsen-Scott South Pole station, are described here. When completed, IceCube will consist of at least 70 strings, each with 60 optical modules. About a cubic kilometer of ice at depths between 1450 m and 2450 m will be instrumented (Figure 1). During the austral summer of 2004-5 the first IceCube string was deployed along with four stations of the surface air-shower array, IceTop. In the following sections we consider the design and performance of these first elements of the IceCube Neutrino Observatory.

II. Design Goals

The goals of the design are to deliver high quality data that contain the maximum amount of useful information from each sensor. The most interesting events are likely to occur very infrequently and their detection and unambiguous reconstruction may require all the information a PMT can deliver. Optical scattering in the deep ice predominates over absorption, which disperses the photon arrival times with increasing distance between source and detection. Thus, the

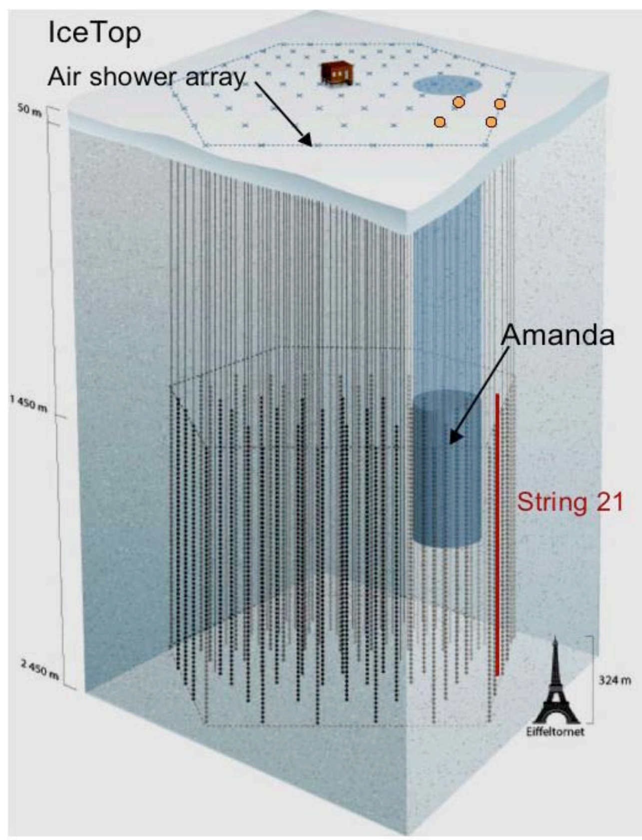

Figure 1: Schematic plan for IceCube and IceTop. The location of the present detector, AMANDA, is indicated as are the first four IceTop stations and the first IceCube string ,"String 21."

ensemble of arrival times contains important information about an event and underscores the importance of waveform capture. At the same time, the location of the detector at a geographically remote site places constraints on power consumption and makes it advantageous to be able to execute complex operational and maintenance functions remotely from the northern hemisphere. The electronics, once deployed in the ice, are forever physically inaccessible - therefore they must be highly reliable. While the electronics located on the surface can be repaired, replaced and upgraded, reliability is important here as well, since the austral working season is limited to mid-November to mid-February. Other logistical factors in transporting equipment to the South Pole also influence the design, as does the cost of producing 5000 of the optical modules.

III. The Design

Much valuable experience in detector design and construction has been gained from AMANDA, the Antarctic Muon and Neutrino Detector Array, which consists of about 650 optical modules on 19 strings [1]. With regard to data acquisition, a variety of technologies were employed in building AMANDA, from the simplest to the fairly complex. A prototype of the IceCube design was deployed by AMANDA as its 18th string in January, 2000. This string included 41 Digital Optical Modules, or DOMs. [2]. This prototype was invaluable for producing the present design, which is based on the concept of the Digital Optical Module, or DOM.

A. Concept

The highest quality data are obtained by recording the PMT waveform locally, which enables digital transmission to the surface. Time stamping the digitized waveform requires that there be a local clock, i.e. a local oscillator, which is calibrated against a master oscillator on the surface. This is accomplished by a custom ASIC waveform digitizer, the Analog Transient Waveform Digitizer (ATWD) in concert with a very stable quartz crystal oscillator. Useful information is enhanced over noise by introducing a hardware local coincidence between neighboring modules. State control, message management, analog calibration, time calibration, monitoring, and other housekeeping functions are enabled by an FPGA + embedded CPU in conjunction with ADCs and DACs. Indeed, the DOM functions as a semi-autonomous mini data acquisition system, which effectively distributes front-end processing tasks throughout the array. Each DOM is connected by a single copper twisted-pair to a surface readout card (the Digital Optical module Readout, or DOR card), which supplies the DOM with power, communications, and analog time calibration signals. The DOR card collects the data from the DOMs and passes it via a standard PCI bus to a CPU in the DOMhub. From the DOMhub the information is moved to a string processor by TCP/IP ethernet and to other processors for software triggering and event building. An overview of the IceCube DAQ system is given in Figure 2.

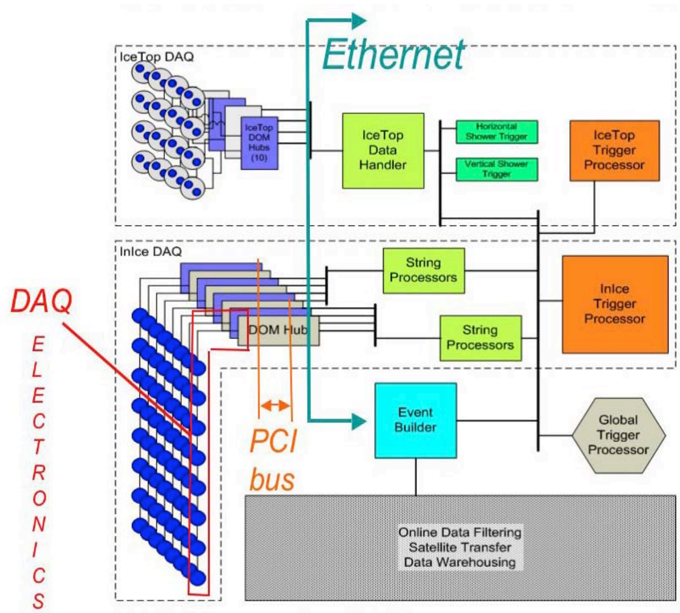

Figure 2: Overview of the DAQ system for IceCube and IceTop

B. The Digital Optical Module

The DOM is the fundamental element of the system. The different components of the DOM and their physical arrangement are shown in schematic form in Figure 3. The PMT is a HAMAMATSU R7081-02 25-cm diameter photomultiplier tube with a spherical photocathode and 10 dynodes. A PMT is operated at a gain of 10^7 at a voltage in the

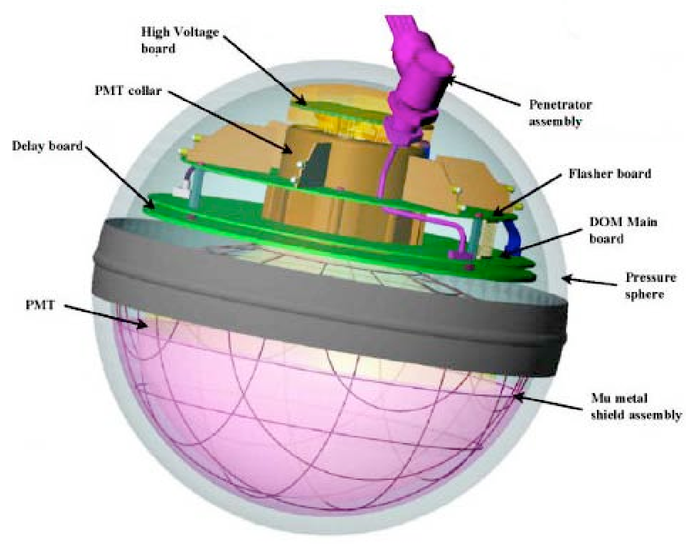

Figure 3: The major components of the DOM

range 1200 - 1400 volts. It rests in a silicone gel, which provides optical coupling to the glass pressure sphere and mechanical support for the PMT and all the electronics, which are supported by the neck of the PMT. A mu-metal wire cage provides magnetic shielding. Four printed circuit boards are arranged concentrically with the tube and glass sphere. From top to bottom in Figure 3: a passive base for distributing high voltage to the PMT anode and dynodes; a "flasher board" having twelve LEDs (405 nm) arranged in six pairs; the PMT HV is generated on a daughter board situated on the flasher board; the mainboard, which contains most of the functionality in the DOM; and a 75 ns delay line, which is fabricated on a PCB of the same size as the mainboard. Communication with the surface is via 0.9 mm copper wire, which penetrates the pressure sphere in a molded assembly. The 13 mm thick glass sphere (from Benthosphere) is able to withstand pressures exceeding 500 bar. At assembly the sphere is evacuated and back-filled with dry nitrogen to a pressure of 0.5 bar.

1) The mainboard

Refer to Figure 4, the mainboard block diagram. The PMT anode signal is coupled to the mainboard input via a transformer, which greatly reduces the energy stored at high voltage compared to conventional capacitive coupling. A discriminator launches the signal acquisition process by triggering the ATWD. This discriminator has a typical rms noise, referred to input, of <100 μV. After a delay of 75 ns the signal enters three input channels, which have gains differing by successive factors of 8. Each signal path feeds an input channel of the ATWD having an input range of 2V. In this manner, a dynamic range of 400 PE/15ns is attained while triggering at a level of 0.25 PE. In addition, a fourth signal path is shaped (30 ns) and fed directly to a 10-bit fADC operating at a sampling speed of 40 MHz. 256 samples are read out following a discriminator trigger, giving 6.4 μsec of acquisition.

Analog Transient Waveform Digitizer

The ATWD is a switched capacitor array with four channels, each 128 samples deep. Once a launch is received, all channels sample synchronously. The sampling speed of the ATWD can be chosen between ~1.6 and ~5 ns/sample, and is currently set at 3.3 ns/sample. This provides 420 ns of high-speed sampling. The first three channels are used for PMT signal. The fourth ATWD channel is used for calibration and monitoring purposes and a variety of signals can be multiplexed to it. For example, by recording the oscillator waveform, a precise measurement of the sampling rate can be made. The discriminator transition is resynchronized by the FPGA to launch the ATWD on the next clock cycle (40 MHz). The resynchronized launch transition also latches a scaler to provide the local coarse time-stamp. The precise time of a signal is determined from the coarse time stamp and the sample number of the ATWD at which the signal appears; fitting the waveform can provide time resolution significantly better than the 3.3 ns sample. Within the ATWD, 128 common-ramp 10-bit Wilkinson ADCs digitize a channel in 30 μs. Thus, if a large anode signal fills all three ATWD input channels, the time to digitize it is about 100 μs. Two ATWDs are used in ping-pong fashion to effectively eliminate any dead time associated with readout. Each ATWD consumes 125 mW.

Local Oscillator

The local oscillator, like the ATWD, is a key component in the DOM system. It is free running and (in a procedure described below) calibrated periodically against a master oscillator on the surface. The frequency stability of this oscillator will determine the repetition rate of the calibration procedure. A frequency stability (Allan variance) of $\delta f/f < 10^{-10}$ in a

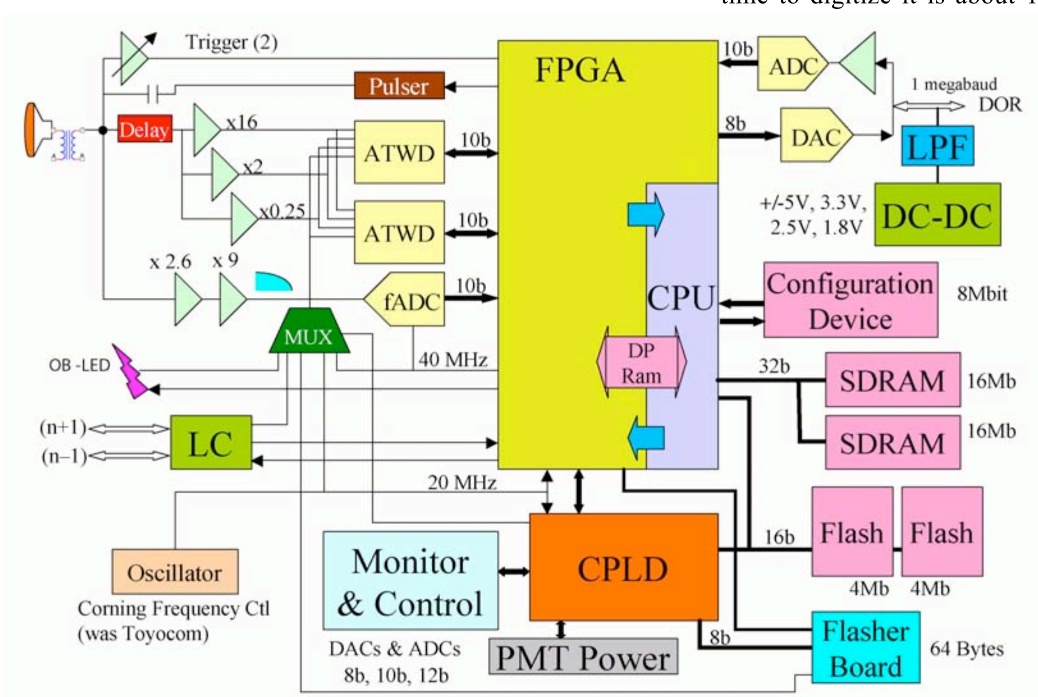

Figure 4: Mainboard block diagram.

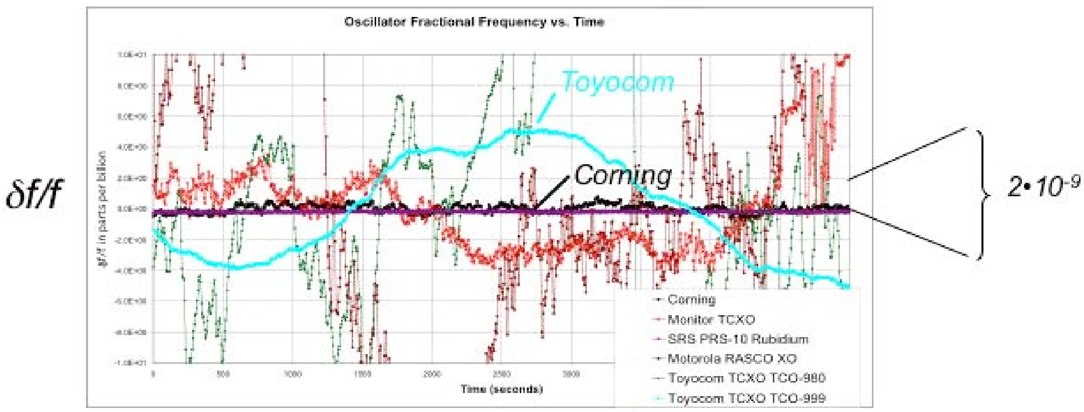

Figure 5: The fractional frequency stability of several oscillators measured over 5000 s. The Toyocom and the Corning have the best short-term stability, which is about 10^{-10}.

3-10 second interval is adequate. Two low-power devices that meet this requirement are a 16.6 MHz crystal oscillator by Toyocom (used in the prototype String 18) and a 20 MHz oscillator by Corning. The latter was chosen because of reliability considerations and the manufacturer's willingness to provide Allan variance screening. Figure 5 shows the Allan variance for the Toyocom and Corning oscillators, and a few other commercial products.

Local Coincidence

The launch rate of the ATWD can be significantly reduced by requiring a time coincidence between neighboring DOMs or next-nearest neighbors. This capability is achieved by connecting each DOM to its neighbor by a dedicated twisted pair. The Local Coincidence can be used in a number of ways to reduce selectively the amount of information transmitted to the surface. In the planned operating mode for IceCube, local coarse time stamps and the highest three contiguous values of the fADC will be recorded for all discriminator launches, which arise mainly from dark noise at typical rate of 700 Hz. Full waveforms will be sent to the surface only for those launches which meet the local coincidence requirement. This rate, which arises from cosmic-ray muons, will be 10-25 Hz, depending on the depth of the DOM and whether the local coincidence can be satisfied by next-nearest as well as nearest neighbors.

Power and Communications

Power, communications, and analog clock-calibration signals are supplied via a single pair of copper wires. A low pass filter on the twisted pair feeds ±40 VDC to a DC-DC converter on the mainboard. Communications and timing signals are transmitted and received by a DAC and ADC, which operate at 20 MHz. The communications signaling rate is 1 Mbaud on the wire pair. (This bandwidth is shared by two DOMs.) The signaling is differential, which provides a high level of common mode rejection. This is an important feature in reducing electromagnetic interference from VLF and radar transmitters at the South Pole, which are used in other research projects. So far, neither the prototype AMANDA digital string nor IceCube's first string have shown any deleterious signs of interference from the ~ 7 kW, 19 kHz VLF transmitter located nearby.

The mainboard distributes power and communications through interfaces defined in the CPLD to the flasher board and HV supply for the PMT base. The HV supply is mounted on the flasher board to prevent noise from the HV DC-DC generator from entering the analog sections of the mainboard. A number of sensors and devices are set and monitored via DACs and ADCs. Some of the quantities monitored are board temperature, internal pressure, HV, and various DC levels. Two calibration devices, an on-board LED and an electronic pulser, are controlled directly by the FPGA. The on-board LED is used to measure the time delay between photo-electron emission from the photocathode and the arrival of the anode waveform at the input of the ATWD. Since this value is dependent on the PMT voltage, it is measured as a function of the HV.

FPGA with embedded CPU

The many functions of the mainboard are enabled and controlled by an FPGA with an embedded CPU. The Altera Excalibur EPXA 4 has 400,000 gates and is clocked at 40 MHz. The CPU is an ARM 32 bit processor and is clocked at 80 MHz. It communicates with the FPGA via dual-port shared memory. This system-on-a-chip provides much capability at a power consumption of only 0.5 - 0.7 W, depending on the tasks being executed. There are three main firmware/software applications that run (separately) on the mainboard; data acquisition (DOMapp), calibration (DOMcal), and a test suite, Simple Test Framework (STF). The code for these is resident in flash memory and loaded at startup. DOMapp and the FPGA collect data from the ATWD and fADC, format and compress it, placing it in a buffer for transmission to surface. Data collection occurs without interruption, independent of data communications and time-calibration. Since time calibration is a repetitive process occurring every 3-10 seconds, this procedure is controlled in firmware on the surface and the time calibration waveforms are transmitted to the surface as a part of the data stream. Other calibration procedures, such as HV gain, charge calibration, and sampling speed are performed infrequently. These calibrations proceed automatically, once started. The STF process, which checks all functionality in the

DOM is run before deployment as a part of testing the modules after arrival at the South Pole and again after deployment to verify that the modules have survived freeze-in.

Firmware and Software

With the exception of a basic boot program that initiates on powering up the DOM, all firmware and software associated with the functions described above can be downloaded to the DOM from the surface. This can be done remotely. Indeed, it is possible in principle to "log in" to a specific DOM from a terminal anywhere (providing the satellite serving the Pole is over the Antarctic horizon). This capability to upgrade firmware and software is a basic requirement for the IceCube electronics.

Developing the firmware and software for the DOM system has been a major effort and is ongoing. (The DOMapp alone contains about 6000 lines of code.) Much of the system code was developed initially to test the first mainboards and DOMs before they left the northern hemisphere. Modifications and adaptations of this code have been incorporated in the DAQ soft/firmware running at the South Pole now. More advanced versions will be installed in preparation for the next deployment season.

C. The Cable

The cable connecting the DOM with the front-end DOR card on the surface is also a key component of the electronics system. Figure 6 shows a cross section of the cable. The cable, DOM penetrator assembly, and cable connections must be immune to the high pressure and stress that arise during the freeze-in process. Since there are 30 pairs of DOMs all communicating independently, cross-talk could be a significant source of errors in communication, the recovery of which necessarily consumes some of the available bandwidth. The time calibration procedure is even more sensitive to cross talk, as the high frequency components of the digital transmission signals could interfere with the analog pulses used for time calibration, thereby effectively introducing noise in the system. Cross-talk suppression requires careful mechanical assembly of the cable, as any mechanical asymmetries or imperfections in the twisted quad configuration introduce cross-talk. (Indeed, one particular quad that experienced some damage during deployment shows a significantly higher bit error rate and noise level "on the wire" than any other quad.) The relevant requirements for the cable are that near-end and far end cross-talk be suppressed by more than 50 db and 30 db, respectively.

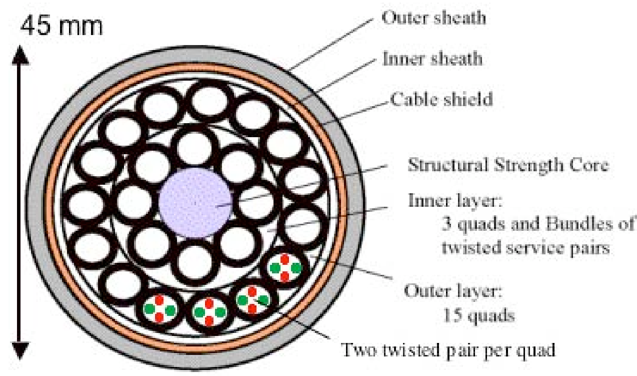

Figure 6: The electrical cable from the DOMs to the DOR card at the surface. Four DOMs are serviced by one twisted quad.

D. The DOR surface readout card

The DOR card is at the surface end of the main cable and provides power, control, and communications for the DOM. In addition the DOR card provides the interface in data flow between the custom-designed electronics of the DAQ and its higher level systems that use commercial standard protocols and off-the shelf components. The block diagram for the DOR card is shown in Figure 7. Each DOR card serves 8 DOMs on two twisted-quad cables. Communications with the DOM are half-duplex in a master/slave relationship. The DOR is constantly polling the DOM for data, and the DOM does not transmit

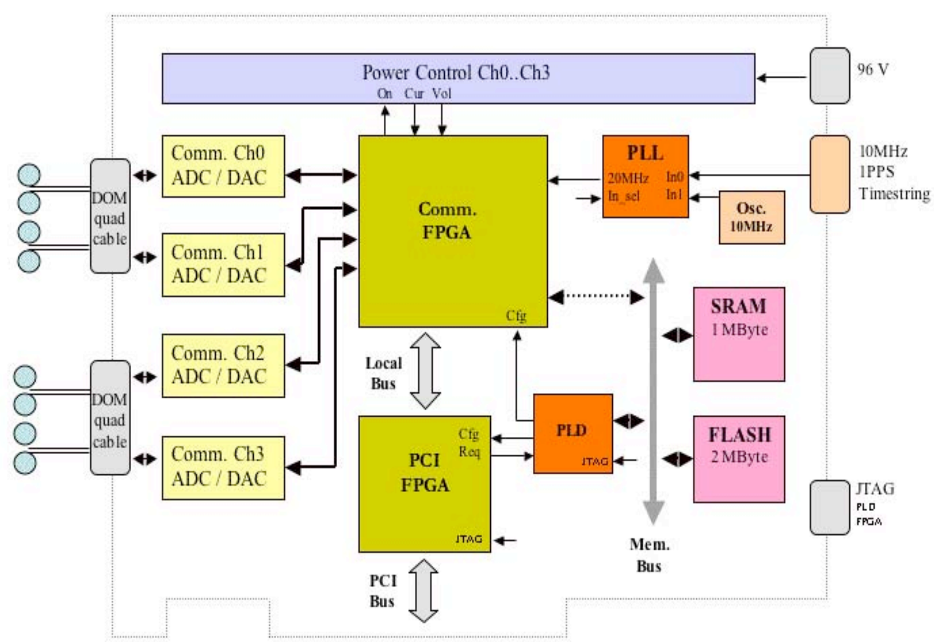

Figure 7: The block diagram for the Digital Optical Module readout card.

unless polled. The DOR mirrors much of the functionality of the communications portion of the DOM mainboard. The DOR FPGA, an Altera EP1C20, controls the communication DACs and ADCs, and frames and deframes the data packets. The signalling rate is 1 Mbaud, which provides an upper limit bandwidth of about 45 Kbytes/s to each DOM on a twisted pair. The time-calibration procedure, controlled at the DOR in firmware, is initiated automatically at regular predetermined intervals, the length of which must depend on the stability of the DOM local oscillator. (Even at a rate of 1 Hz, the time calibration procedure consumes negligible bandwidth.) The main FPGA is clocked at 20 MHz from a signal that is synchronous on all DOR cards and obtained from the master clock distribution system.

The DOR card connects to a PCI bus through a second, smaller FPGA. This bus handles the data flow and higher-level control originating in the DOM Hub CPU. The DOR card consumes 5.5 W or 0.7 W/DOM.

F. The DOM Hub

The DOM Hub is an industrial PC chassis that holds 8 DOR cards, a CPU card, and a clock signal fanout (**D**omhub **S**ervice **B**oard) - all in a PCI bus. The Hub contains two 48 VDC power supplies that supply the ±48 VDC to each twisted pair. The Hub CPU's main software application is the driver that communicates with the DOR card and, through it, with the DOMs. (The driver is about 10K lines of code.) Dual Pentium III processors and 2 GB of RAM require about 70 W. (Next season this CPU will be replaced with a faster processor, which will consume only about 20 W.) The output of the DOM Hub is a TCP/IP Ethernet port, which sends data on to the String Processor, where the local time stamps for each hit are transformed to master clock time and a software "string trigger" can be applied to the individual "hits" from the 60 DOMs on that string. When all 60 DOMs are in normal operation, the DOM Hub uses 300W total, or 5 W/DOM.

IV. Reliability and Testing

The detector must operate for ten years after the completion of construction. This implies at at least 15 years of operation for the strings deployed at the beginning. This requirement has consequences for both the design and for the testing program. All parts must be selected for their ability to work at low temperatures. The lowest temperature in the deep ice is for modules at the upper end of the instrumented portion of the string, and is about -35^{o}C. DOMs in IceTop will experience temperatures at least 10^{o}C colder than this. All parts must therefore be selected with these extreme temperatures in mind. Many parts are available with an industrial rating of -40^{o}C. Those essential parts that are not available (at reasonable cost) with this rating must be tested to establish their reliability.

Extensive testing was the norm in producing the design, in verifying that the design performed as intended, in exploring the limits of operating parameters and, finally, in determining that each and every DOM functions as specified before deployment. Thus, a few mainboards were tested over the temperature range from -80^{o}C to +80^{o}C, and subjected to vibration up to to 30 G rms. All mainboards are tested by power-cycling, rapid temperature cycling (-50^{o}C to +65^{o}C), and exposing them to vibration (7 G rms). Burn-in periods of 24 hours each at -50^{o}C and +65^{o}C are used. The test-application is run during these tests and again afterward. Before being released for assembly in complete DOMs, each mainboard is integrated in an otherwise complete DOM and operated by a DOM Hub connected with a 3.4 km twisted quad cable.

Sound reliability and design practices include parts selection, as mentioned above, and require selection of preferred, qualified vendors to supply the parts. Components should be operated at well below their rated limits (derating). Special attention must be paid to custom components to be sure that they will work properly at low temperatures, and that the foundries and packagers of these parts follow good practice. For the printed circuit boards we require that vendors follow IPC 610 class 3 fabrication procedures. This is the class used for medical and some satellite equipment. Some consequences of this emphasis on reliability were (i) the replacement of electrolytic capacitors with higher-reliability plastic capacitors, (ii) the discovery of some component types that were improperly rated or inadequately tested by their manufacturers, and (iii), the substitution of components that had been used successfully in the prototype string with other components that were better constructed and more extensively tested by the manufacturer. For example, a more expensive and better-constructed crystal oscillator from Corning was substituted for the Toyocom oscillator even though the Toyocom used in String 18 had a slightly better short-term frequency stability.

Fully assembled DOMs are tested at each of the three production facilities (U. Wisconsin, DESY-Zeuthen, and U. Stockholm) by placing them in a large freezer for 14 days over a range of low temperatures and re-running all the STF tests. A laser and fiber optic distribution system is used to verify the time resolution and time calibration of each DOM. After the DOMs have been transported to the South Pole, they are again tested at the ambient surface temperatures (-20^{o}C to -30^{o}C) before they are deployed at depth or frozen in the IceTop tanks.

V. Performance

The deployment of the first IceCube string (60 DOMs) and four surface stations for IceTop (8 tanks containing 2 DOMs each) in January 2005 made possible the verification in situ of the performance of the basic elements of the IceCube Neutrino Observatory [3]. The first power-up and communication with deployed DOMs took place on January 28, 19 hours after the string was lowered to its full depth. Extensive testing of all DOMs began after the freeze-in process was completed over the full length of the string, some two weeks later. All DOMs booted up properly and have continued to function since deployment. The intervening time has been used for debugging and verification and, as a part of this, to take a considerable amount of data using down-going muons. No serious attempt has been made yet to find neutrino events with this single string since, for the present, the verification and testing can be done with cosmic-ray muons and built-in calibration devices. Some of the basic quantities for IceTop and IceCube, such as the noise rates of the PMTs as a function of time after deployment, gain stability, communications bit error rates, and so on, need not be reported here. So far, these characteristics generally look very good (especially the low, 700 Hz noise rates) and the system is quite stable.

A. Time calibration

The phase and frequency of each DOM's free running local oscillator are determined relative to the master oscillator by transmitting bipolar pulses from the DOR card to the DOM, and subsequently, after a known delay, from the DOM to the DOR card. The effects of the long cable on the rise time of the pulse are significant - a rise time of a few nanoseconds becomes a microsecond or more at the other end. The accuracy of the method arises from the reciprocity of the pulsing system [4], in which the generated pulses at each end have the same shape and the disbursed, attenuated received pulses at each end have the same shape. In this limit, the one-way time is equal to one-half the roundtrip time minus the known delay time, regardless of which feature of the waveform (e.g., leading edge or crossover) is taken as the fiducial mark. Reciprocity (or symmetry) is attained because the calibration signals follow the same electronic path through the same components for both transmission and reception. Reciprocity is also verifiable, because the calibration waveforms are digitized in both the DOM and DOR, and these waveforms can be compared to determine any differences in shape.

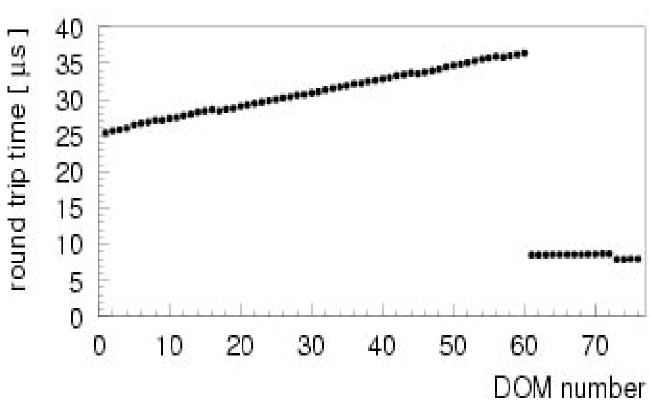

Figure 8: Round trip times for IceCube DOMs (1-60) and IceTop DOMs (61-76).

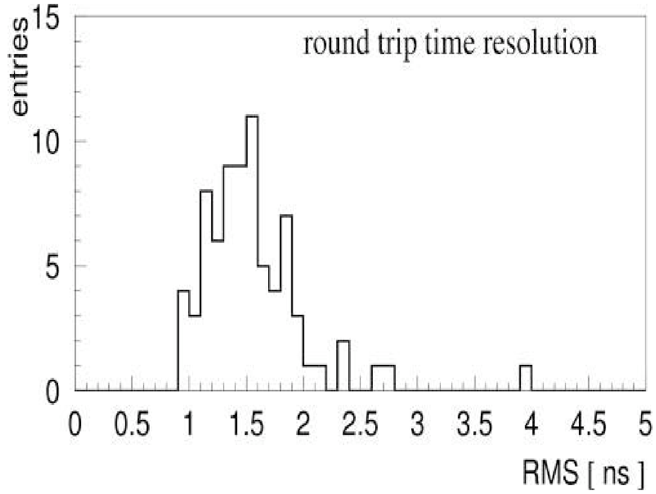

Figure 9: The round trip time resolutions for all 76 DOMs.

The values of the roundtrip times for different DOMs correspond to the electrical length of the cable connecting the DOR and DOM. This is illustrated in Figure 8. The times are larger for progressively deeper sensors on the string (DOMs with numbers 1-60), and are essentially the same for the IceTop sensors (shown as DOMs with numbers 61-76). Calibrations are done automatically every few seconds. The round trip time for a single DOM varies slightly from one calibration to the next, and the size of the variation provides the basic measurement of the precision of the time calibration procedure (Figure 9). The single-shot round-trip resolution is typically less than 3 ns rms; the precision of the mean round-trip time becomes a small fraction of a ns very quickly.

B. Detector verification with flashers

The flashers contained in each DOM are a powerful tool for calibration, for determining the optical properties of the ice, and for measuring the precision of the timing. They are extremely bright (~6×10^9 photons/LED/pulse) and can be seen by optical modules several hundred meters away. Figure 10 shows the variation in time difference for the arrival of leading photons at DOMs 58 and 59 when DOM 60 (at the bottom of the string) is flashing. Since these are intense pulses, single photon statistics and scattering in the ice contribute little to the width of the distribution, which is 1.74 ns. This indicates that the time resolution for a single DOM is aroughly $1.74/\sqrt{2} = 1.2$ ns. The results for all 60 DOMs are shown in Figure 11.

The flashers can reveal the optical properties of the ice as well as demonstrate the timing performance, as is demonstrated in Figure 12, which the shows the arrival time of the first photon in a burst, when DOM 47 is flashing. Since the LED beacons point horizontal and upward, and the PMTs look downward, no photons would be detected in DOMs below no. 47, were it not for optical scattering in the ice. For DOMs above no. 47, the time distributions remain relatively narrow (on this plot) until the fifth DOM at a distance of 85 m above DOM 47. The broadening of the time distributions at large distances due to the scattering is evident here.

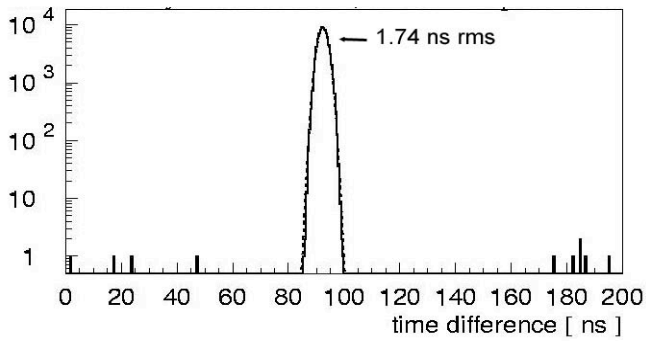

Figure 10: Time difference for photons arriving at DOM 58 and 59, with DOM 60 flashing.

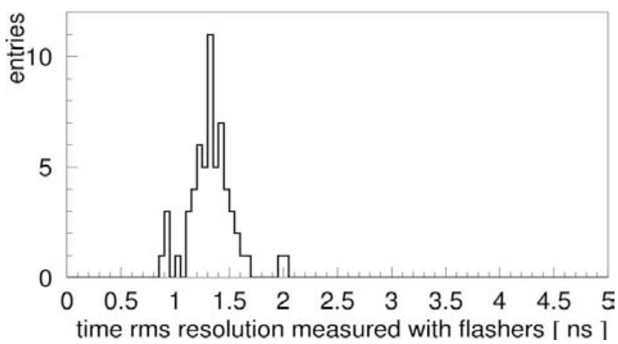

Figure 11: the time resolution obtained for all adjacent pairs of DOMs receiving flasher pulses.

C. Muon reconstruction

A typical ATWD waveform, generated by a cosmic-ray muon, is shown in Figure 13. The waveforms are described very well by a waveform decomposition procedure, which yields single photon hit times. A likelihood minimization algorithm for track reconstruction in multi-layered ice with only one string was used to reconstruct the tracks of down-going muons. The scattering and absorption values used were those measured with AMANDA [5] and extrapolated to deeper ice using available ice core data and data collected by a dust measuring device used during the string deployment. The track-fitting algorithm was tested on a simulated data sample of down going muons and was found to reconstruct it rather well. The rms resolution of the muon track zenith angle reconstruction is 9.7^o with an event hit multiplicity of 8 or more. The resolution improves rapidly as the multiplicity increases (3.0^o at multiplicity 20, and 1.6^o at multiplicity 40). This is similar to the one-string AMANDA analysis results [2]. An example of a high multiplicity event is shown in Figure 14, which also includes a coincidence with the IceTop shower tanks.

D. Timing verification with muons

To measure any systematic time offsets for different DOMs in the IceCube string we applied the one-string reconstruction

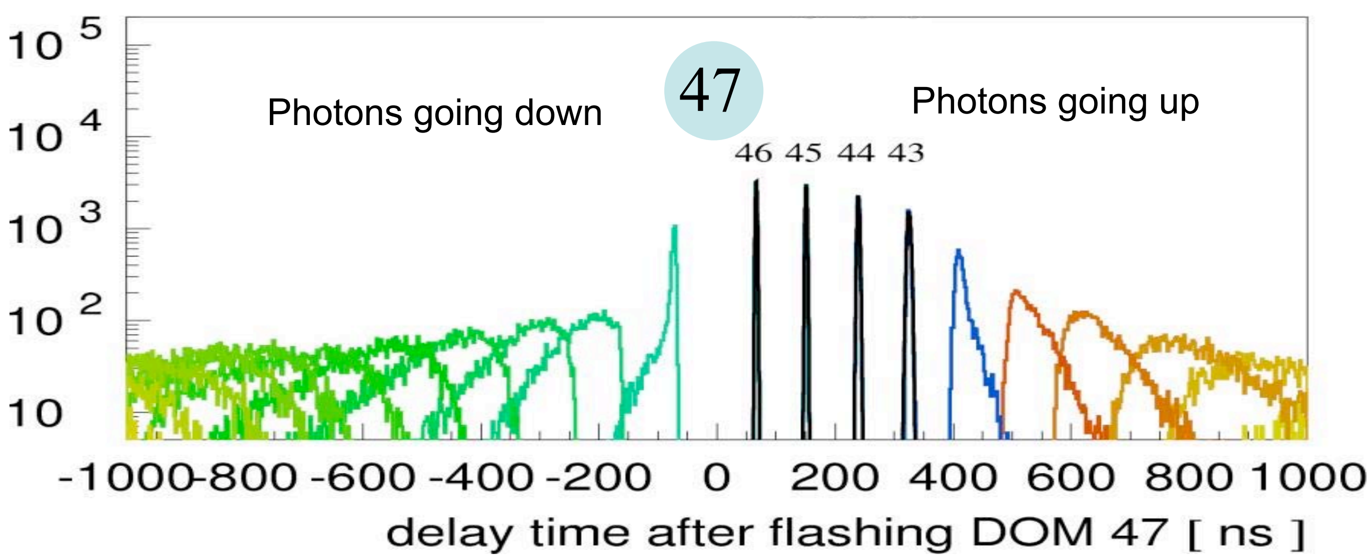

Figure 12: Time delay from flasher burst to arrival of first photon at DOMs above and below the flasher DOM, no. 47.

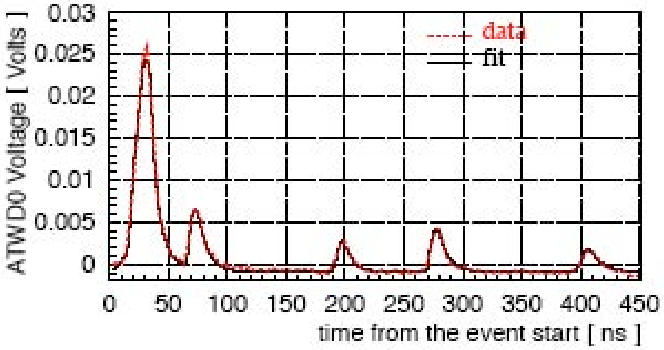

Figure 13: ATWD waveform and the fit used to determine photon arrival times.

to one day's worth of data 60 times. Each of the 60 DOMs was removed once during the reconstruction, and the residual time difference of the actual hits in those DOMs and the expected *direct* (*unscattered*) hit times from the reconstructed tracks were evaluated. The residual time distributions are consistent with the expected distribution of hits coming from nearby muons (Figure 15). The maxima of such distributions indicate the time residuals of the most probable hits. In addition to systematic electronic time calibration offsets these can be systematically displaced from zero due to still-unaccounted-for features of the DOM geometry as deployed and optical scattering due to dust layers, which may affect photon propagation even at small distances. Most of these residuals are within 3 ns of each other, except for DOMs 35-43, which are located in dustier ice (Figure 16 top and bottom). This indicates that the DOM clock times for the whole array (currently 76 DOMs) are calibrated to within 3 ns of each other. An apparent large time offset, -10 ns, for DOM 60 is still under investigation.

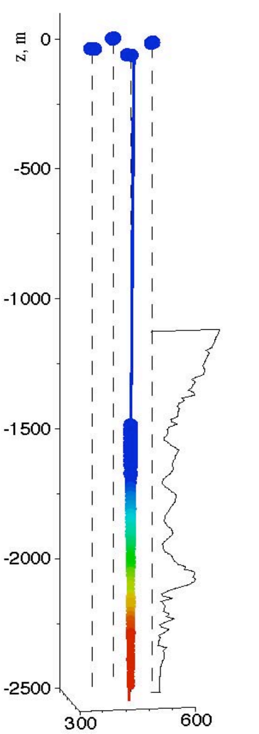

FIG. 14 An IceCube event in which all modules received a hit. The curve denotes the effective scattering coefficient of the ice.

E. Coincidence events

1) IceCube - IceTop

Figure 14 shows a high multiplicity event in which all IceTop tanks and all DOMs registered hits. Data such as these can be used to determine the zenith angle distributions for air showers and for the coincident muons observed deep in the ice.

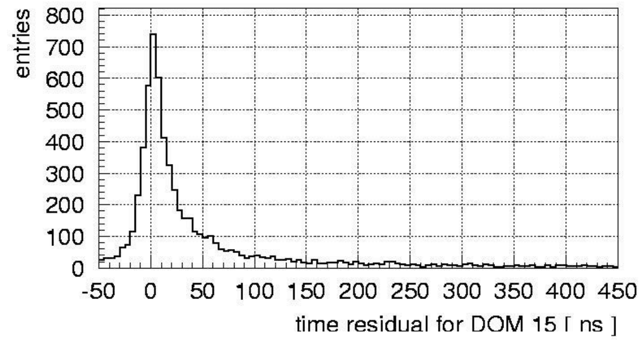

Figure 15: Distribution of time residuals between the hits recorded by a DOM and time expectation for direct (unscattered) hits from nearby tracks reconstructed with the rest of the string.

Coincident deep-ice and IceTop events with a combined hit multiplicity of at least 14+14 hits collected during March, April, and May were analyzed with both the IceTop shower reconstruction and the one-string muon track reconstruction discussed above. The resulting zenith angle distributions are compared in Figure 17. The directions obtained with the string reconstruction seem to be systematically closer to the vertical, which may indicate the need to improve the likelihood

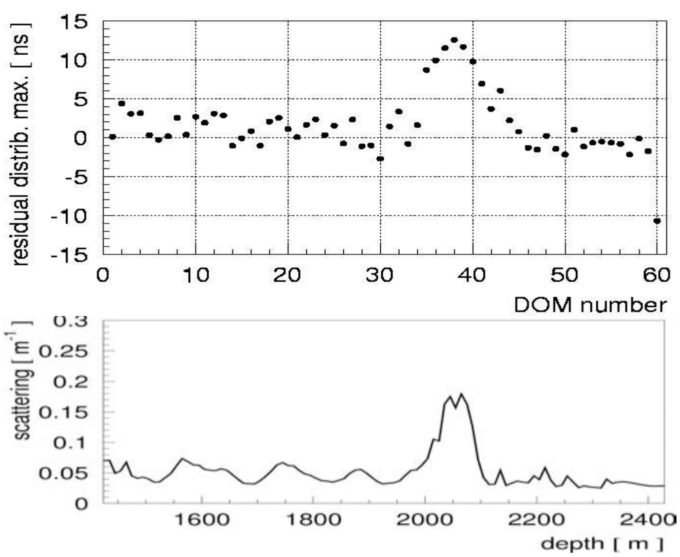

Figure 16 top: Distribution of direct hit time residuals for all DOMs on the string. bottom: the scattering coefficient for ice at the depth of the 60 modules. This is the origin of the peak between DOMs 33 and 43.

parameterization used in the track reconstruction. Alternatively it may be due to the air shower front being curved and muons originating from a different part of the shower than that seen by IceTop. We measure a systematic offset of 2.1^{o} with an rms deviation of 4.1^{o}.

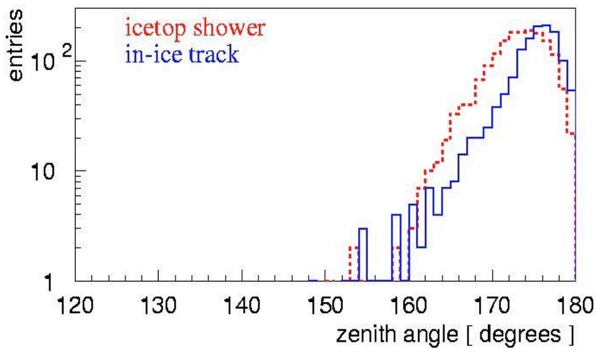

Figure 17: Zenith angle distributions for air shower events and for the associated muons observed with the IceCube string

2) IceCube - AMANDA

Events observed simultaneously in the IceCube and the AMANDA arrays will be identified through comparing the absolute GPS times of the events in each array. At the moment, the first IceCube string lies well outside AMANDA (Figure 1), but it has been possible to find a few relatively horizontal muons that intercept the IceCube string and the AMANDA array (Figure 18).

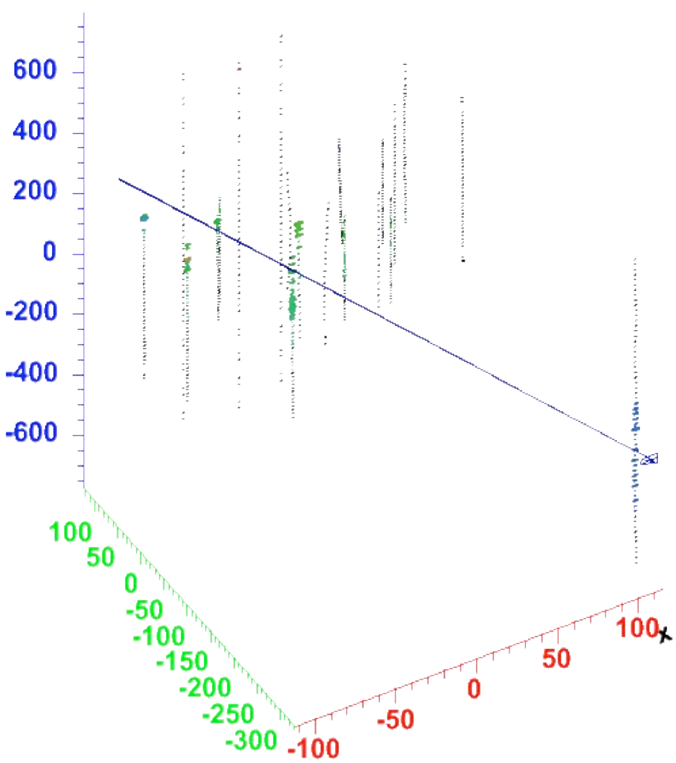

Figure 18: An AMANDA - IceCube coincidence.

VI. Summary and Outlook

The performance of the IceCube electronics *in situ* has been examined using the first IceCube string of 60 DOMs and 16 IceTop DOMs. All 76 DOMs are functioning well and the system meets or exceeds the design requirements. The resolution of the time calibration system is typically 2 ns. An analysis of cosmic-ray muon events indicates that the overall accuracy relative to the master clock, including any systematic time offsets among DOMs is 3 ns or less with one exception (DOM 60). Multiplicity distributions and zenith angle distributions for muons observed in the deep ice array have been measured and they are in reasonable agreement with simulations. Coincidences between IceCube and IceTop, and between IceCube and AMANDA have been observed. As a result of this performance, only very minor changes in the electronics hardware are foreseen for subsequent years. The outlook is to deploy up to 10 strings (along with the corresponding IceTop stations) in the coming austral summer. Thereafter the number of strings deployed per season will rise to 16-18 strings until a minimum of 70 (or maximum of 80) strings are deployed. The search for neutrino events with IceCube will begin after this coming season's deployments, at which time the number of modules in IceCube will be comparable to those in AMANDA.

Acknowledgements

This research was supported by the following agencies: Deutsche Forschungsgemeinschaft (DFG); German Ministry for Education and Research; Knut and Alice Wallenberg Foundation, Sweden; Swedish Research Council; Swedish Natural Science Research Council; Fund for Scientific Research (FNRS-FWO), Flanders Institute (IWT), Belgian Federal Office for Scientific, Technical and Cultural affairs (OSTC), Belgium. UC-Irvine AENEAS Supercomputer Facility; University of Wisconsin Alumni Research Foundation; U.S. National Science Foundation, Office of Polar Programs; U.S. National Science Foundation, Physics Division; U.S. Department of Energy.

References

[1] E. Andres, et al., *Nature* **410**, 441 (2001)

[2] M. Ackerman, et. al., Submitted to NIM, July 2005

[3] D. Chirkin, for the IceCube Collab., Proc. 29th ICRC Pune (2005)

[4] R. Stokstad, et al., LBNL-43200 (1998)

[5] P. Askebjer, *Appl. Opt.* **36**, 4168 (1997); J. Ahrens, et al., *NIM* **A524** 169 (2004)